The effect of CT-based attenuation correction on the automatic perfusion score of myocardial perfusion imaging using a dedicated cardiac solid-state CZT SPECT/CT

John A. Kennedy, PhD,[a,b] Yafim Brodov, MD, PhD,[a] Adam L. Weinstein, MD,[c] Ora Israel, MD,[a,c] and Alex Frenkel, PhD[a]

[a] Department of Nuclear Medicine, Rambam Health Care Campus, Haifa, Israel
[b] Faculty of Biomedical Engineering, Technion, Israel Institute of Technology, Haifa, Israel
[c] B. and R. Rappaport School of Medicine, Technion, Israel Institute of Technology, Haifa, Israel

Received Feb 12, 2017; accepted Apr 18, 2017
doi:10.1007/s12350-017-0905-0

Background. **Data regarding cardiac cadmium-zinc-telluride (CZT)-specific augmented databases and their impact on CT-based attenuation correction (AC) perfusion scores in myocardial perfusion imaging (MPI) were obtained on a multiple-pinhole CZT SPECT/CT.**

Methods and Results. **Summed stress (SSS) and rest scores (SRS) were measured using automated software in three independent patient groups: group 1 ($n = 80$) underwent MPI on both CZT and conventional sodium iodide (NaI) devices, group 2 ($n = 80$) with low coronary artery disease likelihood and normal MPI provided reference CZT databases; and group 3 ($n = 152$) served to compare AC and non-AC (NAC) scores on CZT. Group 1 CZT and NaI scores gave a significant 1:1 linear correlation for CZT scores referenced to the custom database vs NaI scores referenced to the default database, but these were not concordant when CZT scores were referenced to the default database. AC significantly decreased average SSS and SRS in men vs NAC, 4.29 ± 6.30 vs 5.37 ± 7.26 ($P < 0.001$) and 2.37 ± 4.72 vs 3.13 ± 5.85 ($P < 0.001$), but not in women, 2.28 ± 3.42 vs 2.28 ± 3.08 (p NS) and 0.46 ± 1.51 vs 0.61 ± 1.86, (p NS), respectively.**

Conclusions. **Specifically designed databases for solid-state CZT cardiac SPECT provide accurate quantitation of perfusion scores concordant with those previously validated for conventional SPECT. AC and NAC CZT scores differed significantly, especially in men. (J Nucl Cardiol 2019;26:236–45.)**

Key Words: Instrumentation: SPECT • myocardial perfusion imaging: SPECT • cadmium-zinc-telluride • ultrafast cardiac gamma camera • summed stress score

Abbreviations

AC	Attenuation correction
CAD	Coronary artery disease
CTAC	Computed tomography-based attenuation correction
CZT	Cadmium-zinc-telluride
MPI	Myocardial perfusion imaging
NAC	No attenuation correction
NaI	Sodium iodide
SPECT	Single-photon emission computerized tomography
SRS	Summed rest score
SSS	Summed stress score

Electronic supplementary material The online version of this article (doi:10.1007/s12350-017-0905-0) contains supplementary material, which is available to authorized users.

The authors of this article have provided a PowerPoint file, available for download at SpringerLink, which summarises the contents of the paper and is free for re-use at meetings and presentations. Search for the article DOI on SpringerLink.com.

Reprint requests: John A. Kennedy PhD, Department of Nuclear Medicine, Rambam Health Care Campus, P.O.B. 9602, Haifa, 31096, Israel; *j_kennedy@rambam.health.gov.il*

1071-3581/$34.00

Copyright © 2017 American Society of Nuclear Cardiology.

See related editorial, pp. 246–249

INTRODUCTION

Myocardial perfusion imaging (MPI) using single-photon emission tomography (SPECT) is an essential tool in diagnosis of coronary artery disease (CAD).[1,2] Recently, dedicated cardiac SPECT cameras with high sensitivity and resolution have been developed.[3] Such sensitive cameras can perform MPI studies over a very short period of time, or, alternatively, they have the potential of substantially reducing the amount of administered radiotracer with subsequent decrease in patient exposure[4,5] while also coping with potential radiotracer shortages.[6] In place of the scintillating crystal and photomultipliers in conventional systems, these cameras employ solid-state cadmium-zinc-telluride (CZT) detectors with a direct transfer of gamma photon energy to charge creation close to the position of electronic detection. Therefore, the energy and spatial resolution[7] are improved compared to the indirect conversion found in a conventional system.

One of the major advantages of SPECT MPI is its ability for precise automated quantitation of myocardial radiotracer uptake.[8] The value of the total perfusion deficit (TPD) as a measure of extent and severity has been established for both conventional[9,10] and for CZT SPECT systems.[11] An agreement with respect to extent and total severity score[12] and to total perfusion deficit has been found.[13,14] The diagnostic and predictive value of the severity of myocardial perfusion defects assessed by the summed stress (SSS) and rest score (SRS) has been established in conventional SPECT system using sodium iodide crystal detectors (NaI).[15] However, there are no comprehensive studies demonstrating an agreement between the automated perfusion scores obtained from the multi-pinhole CZT device and NaI MPI-SPECT studies. Furthermore, computed tomography (CT)-based attenuation correction (CTAC) is extensively used for the correction of diaphragmatic attenuation in patients undergoing SPECT MPI, while its efficacy for breast artifacts remains unproven.[16] Although the effect of AC used in CZT devices on image quality has been previously compared to a NaI camera,[17] the impact of AC on the automated quantitation of perfusion scores in multi-pinhole CZT cameras has not been yet detailed.

The objectives of the present study were to compare the automated measurements of CZT and NaI perfusion scores of SPECT MPI, to define whether there is a necessity of an augmented database specific to CZT devices, and to characterize the impact of CTAC on CZT-measured perfusion scores.

MATERIALS AND METHODS

Patient Population and Protocol

Baseline characteristics of the study cohort ($n = 312$) are presented in Table 1. Group 1 including 80 consecutive patients were evaluated to compare the automated scores calculated from studies performed on both the CZT (Discovery 570c, GE Healthcare) and NaI (Ventri, GE Healthcare) SPECT cameras. These patients were referred for clinically indicated SPECT MPI and had an intermediate-high pretest probability of CAD.[18] They gave their informed consent to be scanned on both devices following institutional review board (IRB) approval. Group 2 included an additional 80 patients both sexes, with no prior CAD, referred to clinically indicated MPI for atypical (non-anginal) chest pain with no or one major cardiovascular risk factor, considered as a low pretest probability for CAD by Diamond and Forrester criteria,[19] and had a normal MPI study. They were scanned on the CZT device only and served as a reference population for automated scoring providing gender specific and separate AC and non-AC (NAC) databases. Group 3 consisted of 152 consecutive patients with intermediate to high pretest probability of CAD. Their studies were analyzed retrospectively (with IRB approval) in order to determine the impact of CTAC on MPI studies performed with the CZT device. All three groups were independent.

A one-day rest/stress imaging protocol was performed. At rest 10 mCi (370 MBq) of technetium-99m (Tc-99m) tetrofosmin was injected intravenously. Intravenous dipyridamole (140 mg/kg/minutes during 4 minutes) and treadmill exercise Bruce protocol in 189 and 123 patients, respectively, was performed. A standard dose of 30 mCi (1,110 MBq) of Tc-99m tetrofosmin was injected at 8 minutes into the pharmacologic stress and at peak of exercise test. For Group 1, 73 patients had a CZT rest SPECT followed by the NaI scan with a mean delay of 15.6 ± 8.8 minutes (mean ± standard deviation). In seven patients, the NaI rest scan preceded the CZT study with mean delay of 20.0 ± 2.9 minutes between systems. Stress CZT acquisitions were performed before the NaI SPECT in all 80 Group 1 patients at an interval of 13.9 ± 4.6 minutes between systems.

Study Acquisition

The rest and stress acquisition times on CZT were 5 and 3 minutes, respectively, each providing 19 cardio-centric projections (32 × 32 matrix, 2.46 mm pixel size). The camera design has been previously described in detail.[7] Images were reconstructed with the manufacturer's modified 3D maximum-likelihood expectation maximization (MLEM) algorithm on a dedicated Xeleris workstation (GE Healthcare, Tirat HaCarmel, Israel),[7,20,21] using the manufacturer's recommended parameters. Reconstruction for clinical imaging comprises 40 iterations for rest, 50 iterations for stress, with regularization, a 70 × 70 matrix with 50 transverse slices, a 4 mm voxel size, and Butterworth post-filtering (order 7, cutoff frequency

Table 1. Population baseline characteristics

Variable	Group 1 (n = 80)	Group 2 (n = 80)	Group 3 (n = 152)
Age (years)	63 ± 11	56 ± 11	64 ± 13
Male	52 (65)	40 (50)	91 (60)
BMI (kg/m^2)	29 ± 5	29 ± 6	29 ± 5
Chest pain	40 (50)	19 (24)	48 (32)
Hypertension	58 (73)	41 (51)	110 (72)
Diabetes	32 (40)	11 (14)	63 (41)
Smoking	25 (31)	25 (31)	33 (22)
Dyslipidemia	61 (76)	44 (55)	114 (75)
Congestive heart failure	3 (4)	0 (0)	0 (0)
Atrial fibrillation	6 (8)	0 (0)	4 (3)
Pacemaker	1 (1)	0 (0)	2 (1)
Myocardial infarction	16 (20)	0 (0)	45 (30)
CABG	6 (8)	0 (0)	13 (9)
PCI	20 (25)	0 (0)	46 (30)

Age and BMI are expressed as mean ± SD. Other values are expressed as number of cases (% in brackets)
BMI, body mass index; *CABG*, coronary artery bypass grafting; *PCI*, percutaneous coronary intervention; *SD*, standard deviation

0.37 cm^{-1}). The acquisition times for NaI SPECT were 25 and 20 minutes, respectively, with no resolution recovery reconstruction (matrix 64 × 64, L-mode, 60 stops every 3°, 6.8 mm pixel size, low-energy high-resolution collimator). Images were reconstructed using a maximum-likelihood expectation maximization[22] algorithm (2 iterations, 10 subsets; transaxial pixel size, 3.4 mm). The studies were processed on the dedicated workstation included filtering (Butterworth; cutoff frequency, 0.4 cm^{-1}; order, 10 for rest and cutoff frequency, 0.52 cm^{-1}; order, 5 for stress). For both systems, data were electrocardiogram-gated into eight bins and reconstructed data were resampled along the short, vertical long, and horizontal long axes for display. Attenuation correction was not applied, unless otherwise stated. The CTAC scan was performed without moving the patients from the scanning table for either rest or stress SPECT scan (120 keV; 20 mAs; 0.969:1 pitch 5.0 mm slice thickness, helical). All CTAC scans were checked for misregistration with SPECT MPI and re-registered using dedicated software as required.[23]

Quantitative Score Analysis

The SSS and SRS were measured using 17 segments on the Quantitative Perfusion SPECT (QPS) software (Cedars-Sinai Medical Center). The default reference QPS databases for NaI studies were supplemented by the specially constructed databases for the low CAD risk Group 2 population for the CZT SPECT studies. All scoring matched gender, NAC, and AC results with gender-specific NAC and AC databases, respectively. Automated scoring of each segment was performed using a five-point scale heuristically determined to simulate visual assessment: normal uptake (score 0), mildly reduced (score 1), moderately reduced (score 2), severely reduced (score 3), or no uptake (score 4) as compared to the normal database (Figure 1).[15] Scores were automatically summed to yield the SSS and SRS. Changes in the SSS or SRS category were defined as ≤3 normal, 4-8 mildly abnormal, 9-13 moderately abnormal, and ≥14 severely abnormal.[15] Score categories were recorded in relationship to ''improvement'' (lower score) or ''deterioration'' (higher score) when comparing the CZT vs NaI measurements in Group 1 or when comparing AC vs NAC in Group 3. In addition, the CZT measurements for Group 1 were repeated but referenced to the default QPS databases (used as a rule for NaI studies), instead of the specially constructed CZT databases in order to check whether CZT and NaI measurements were concordant without the need of a custom CZT database.

Statistical Analysis

SSS and SRS between the CZT and NaI devices were compared using the Wilcoxon test and linear regression analysis. Changes in SSS or SRS categories with respect to ''improvement'' or ''deterioration'' were assessed using χ^2 test. SSS and SRS for the AC vs NAC results were compared using the Wilcoxon test. Gender differences in perfusion score, BMI, and level of stress were assessed using the Mann-Witney test as were differences in perfusion scores due to type of stress and BMI category. Gender differences in the summed score category and type of stress were assessed using the χ^2 test. A P value < 0.05 was considered as statistically significant.

RESULTS

Validation of Normal Database

When using the custom database for CZT studies and the default database for NaI studies, plots of scores on CZT vs NaI MPI and Bland-Altman plots show that

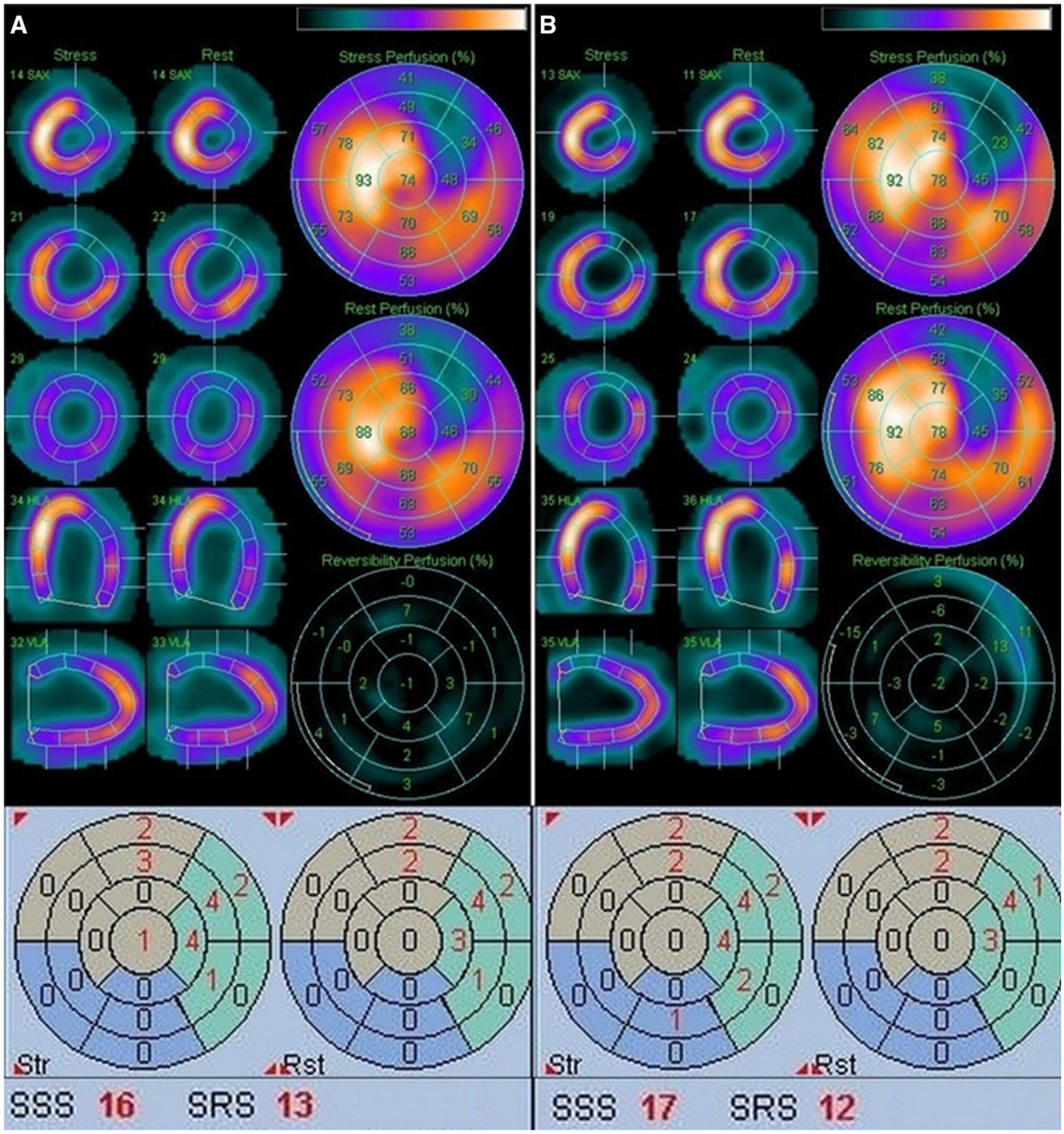

Figure 1. Example of SSS and SRS scoring by QPS software on NaI (**A**) and CZT (**B**). The MPI studies on the NaI and CZT both show a defect in the anterior wall and the scores agree to within ±1. The CZT scoring is referenced to a custom database.

there was a 1:1 linear correlation, without bias, for both the SSS and SRS measurements (Table 2; Figure 2). There was no significant difference in average SSS and SRS between studies performed on the two cameras (Table 3). SSS changed categories in 19% studies (15/80) between CZT and NaI measurements (Figure 3A) referenced to their corresponding databases. This change was by >1 category in 2.5% (2/80) of studies, both patients exhibiting known MPI artifacts (breast attenuation on NaI in one and truncation on CZT in the second). There was no significant difference between the number of studies with ''improvement'' or ''deterioration'' (8/15 vs 7/15, p NS). SRS changed in 13% studies (10/80), all by 1 category and none by >1 category, between CZT and NaI measurements referenced to their corresponding databases (Figure 3B).

When CZT scoring was referenced to the default NaI database, the CZT vs NaI linear fit results were not concordant, as the intercept was non-zero, indicating a significant bias (Table 2). Referred to the default NaI database, average CZT summed scores were significantly larger than corresponding NaI results (Table 3).

Table 2. CZT vs NaI Perfusion scores linear fit parameters for CZT referenced to custom and standard databases

Summed Score	Fitting parameter	Ideal value	Custom CZT database value ± 95% CI	Standard database value ± 95% CI
SSS	Slope	1	0.92 ± 0.13	0.92 ± 0.17
	Intercept	0	0.19 ± 0.79	2.11 ± 1.06[a]
	R	1	0.852	0.774
SRS	Slope	1	0.99 ± 0.10	1.11 ± 0.12
	Intercept	0	−0.14 ± 0.44	0.75 ± 0.53[a]
	R	1	0.917	0.907

All values are mean ± SD. *CI*, Confidence interval; *SSS*, Summed stress score; *SRS* summed rest score
[a] Differs from ideal value

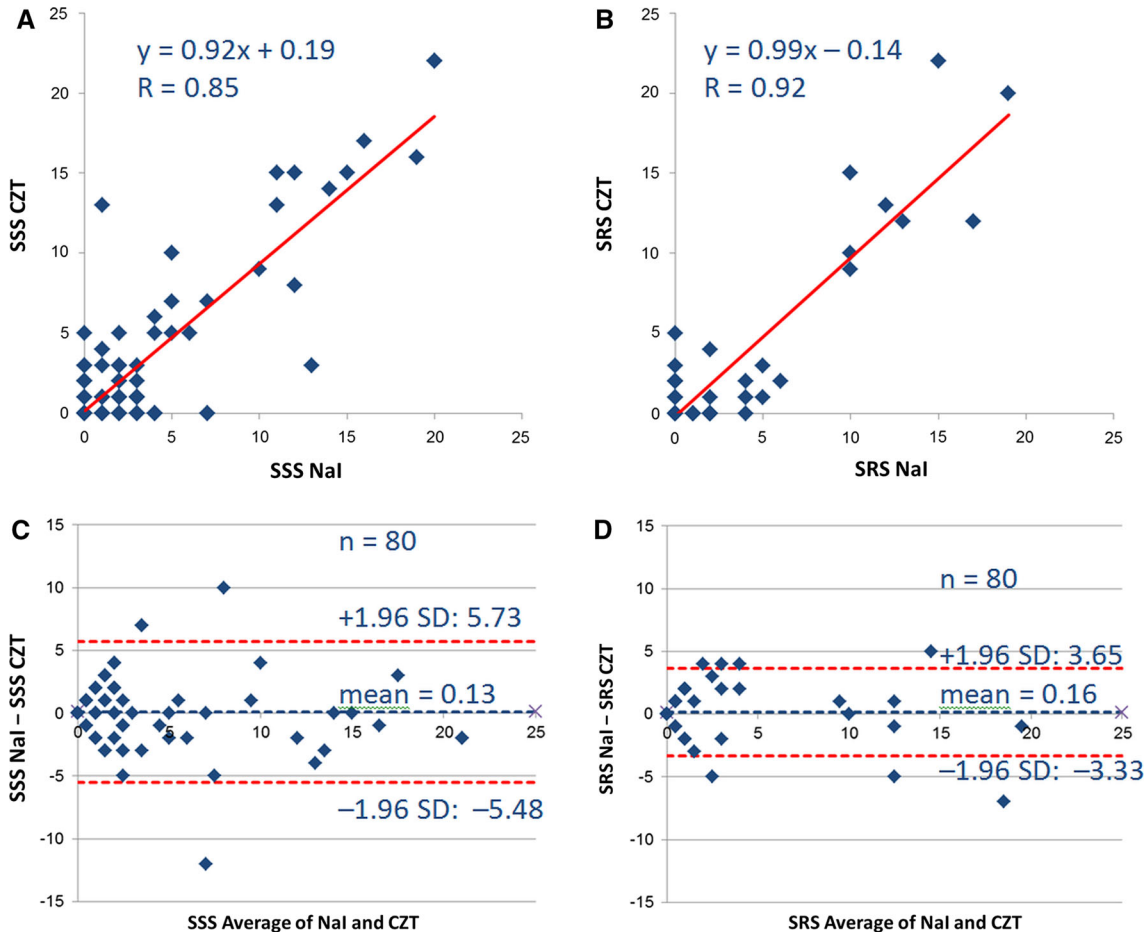

Figure 2. Comparison of summed scores measured on CZT vs NaI for SSS (**A**) and SRS (**B**) showing a 1:1 correlation. Some points overlap ($n = 80$). In Bland-Altman plots, both stress (**C**) and rest (**D**) indicate no bias or proportional error and the 95% confidence intervals fall within ±1 category change.

Both SSS and SRS measured on CZT studies, referenced to the default NaI database and compared to NaI scores (Figure 3C, D), showed significantly more studies which ''deteriorated'' than ''improved'' (27/32 vs 5/32, $P < 0.001$ for SSS, and 12/16 vs 4/16, $P = 0.005$ for SRS).

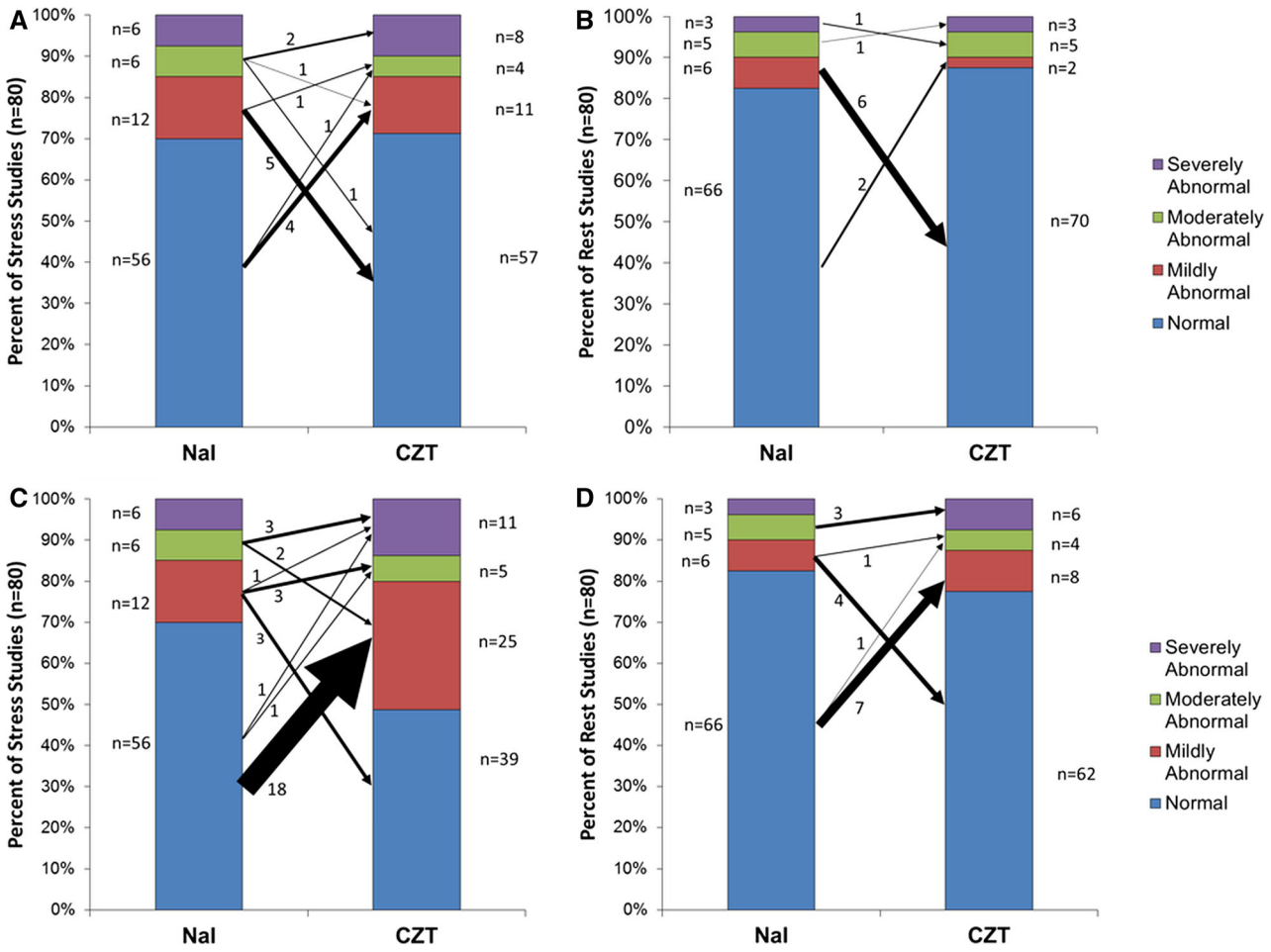

Figure 3. Changes in summed stress and rest score categories between NaI and CZT showing greater agreement in SSS (**A**) and SRS (**B**) if the CZT is referred to the custom database, and greater discordance in SSS (**C**) and SRS (**D**) if the CZT is referred to the default database.

Table 3. Comparison of perfusion scores between NaI and CZT for CZT referenced to custom and standard databases

Summed score	NaI Mean ± SD	CZT with custom database		CZT with standard database	
		Mean ± SD	*P*-value[a]	Mean ± SD	*P*-value[a]
SSS	3.76 ± 5.02	3.64 ± 5.41	N.S.*	5.56 ± 5.95	<0.0001
SRS	1.95 ± 4.15	1.78 ± 4.47	N.S.	2.91 ± 5.06	0.0002

* No significant difference between NaI and CZT results
[a] Compared to NaI results

Effect of CTAC on Scoring

CTAC significantly decreased the average SSS and SRS compared to measurements in NAC studies in men but not in women (Table 4). Males scored higher SSS and SRS values than females, statistically significant for SSS NAC and SRS only (Table 4). In Table 4, there were no significant gender differences (male vs female) with respect to BMI (28 ± 4 vs 30 ± 6 kg/m^2), type of stress (55 of 91 vs 42 of 61 pharmaceutical stress), and level of exercise (percent target heart rate: 89% ± 6% vs 91% ± 5%).

Table 4. NAC and AC Scoring averages for CZT referenced to custom database

	All (n = 152)	Male (n = 91)	Female (n = 61)	P[a]
SSS NAC	4.13 ± 6.12	5.37 ± 7.26	2.28 ± 3.08	0.025
SSS AC	3.48 ± 5.41	4.29 ± 6.30	2.28 ± 3.42	N.S.*
P[b]	0.003	<0.001	N.S.	
SRS NAC	2.12 ± 4.83	3.13 ± 5.85	0.61 ± 1.86	0.002
SRS AC	1.61 ± 3.88	2.37 ± 4.72	0.46 ± 1.51	0.001
P[b]	<0.001	<0.001	N.S.	

NAC, No attenuation correction; *AC*, attenuation correction
* No significant difference
[a] *P*-value comparing male and female
[b] *P*-value comparing NAC and AC

Table 5. AC-induced scoring category changes for CZT referenced to custom database

	All (n = 152)	Male (n = 91)	Female (n = 61)	P[a]
SSS no change	115 (76)	66 (73)	49 (80)	N.S.*
SSS "improvement"	28 (18)	21(23)	7 (11)	N.S.
SSS "deterioration"	9 (6)	4 (4)	5 (8)	N.S.
P[b]	<0.001	<0.001	N.S.	
SRS no change	142 (93)	81 (89)	61 (100)	<0.01
SRS "improvement"	10 (7)	10 (11)	0 (0)	N.S.
SRS "deterioration"	0 (0)	0 (0)	0 (0)	N.S.
P[b]	<0.001	<0.001	N.S.	

Values are expressed as number of cases (% in brackets)
* No significant difference
[a] *p*-value comparing male and female
[b] *p*-value comparing "improvement" and "deterioration"

In male patients, significantly more studies ''improved'' than ''deteriorated'' in the SSS and SRS category with AC (21/91 vs 4/91, $P < 0.001$ and 10/91 vs 0/91, $P < 0.001$, respectively, Table 5). In female patients, there were no changes in SRS category and there was no significant difference between the numbers improving or deteriorating SSS categories with AC (7/61 vs 5/61, Table 5). The most common category change induced by AC for both SSS and SRS was from ''mildly abnormal'' to ''normal'' (26/47, Figure 4).

There was no significant difference in average SSS and SRS between subcategories of low and high BMI (<30 vs ≥30 kg/m^2) or due to type of stress (Table 6).

DISCUSSION

Using the data referenced to the newly built custom database, CZT-MPI perfusion scores were concordant with those obtained for NaI-MPI studies using the default database. These scores were, however, discordant if both the CZT and NaI data were referenced to the default database. The 1:1 linear fit without bias for CZT vs NaI perfusion scores obtained using the custom CZT database for Group 1 is a result that could not be reproduced using the default database. Furthermore, the agreement in the average summed scores between CZT and NaI using the custom database was not obtained with the default database. Referencing to the default NaI database for CZT scoring causes significantly more studies to exhibit an SSS category difference between CZT and NaI, with a bias toward ''deterioration.'' Dedicated ultrafast cameras typically have acquisition geometries and projection data significantly different from conventional systems[24,25] and the present study results indicate that patterns of normal uptake on CZT-MPI studies differ from those obtained using a conventional system to a degree that justifies the need for suitable custom-constructed databases.

On a patient-by-patient analysis, the results obtained in Group 1 were consistent and in the vast majority of studies showed a difference of not more than 1 category in perfusion scoring between CZT and NaI.

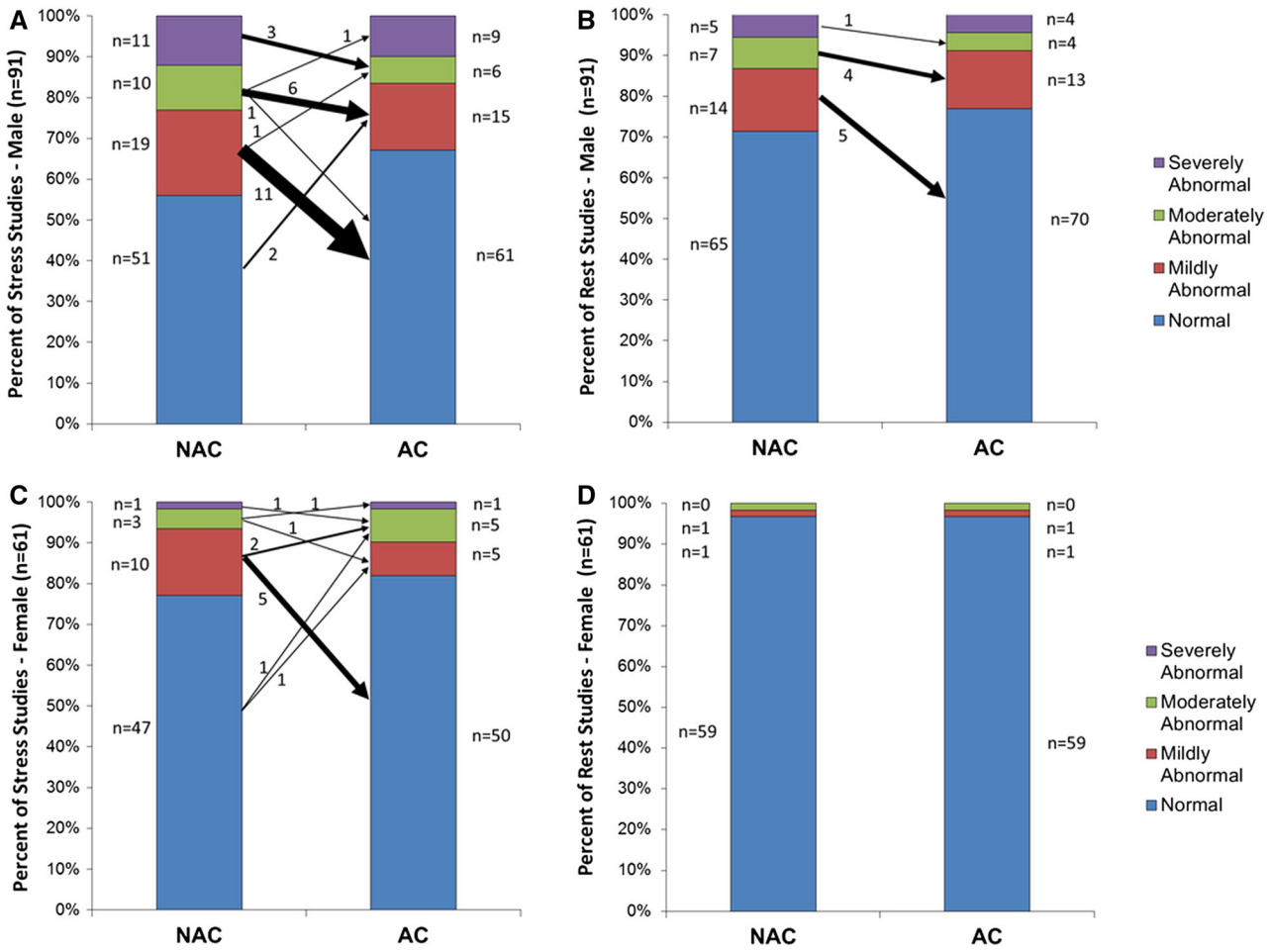

Figure 4. Changes in summed stress and rest score categories between NAC and AC for the CZT referenced to the custom database. **A** SSS males. **B** SRS males. **C** SSS females. **D** SRS females.

In 2 exceptional cases, the disagreement was by 2 categories. In one case, a male stress result was re-categorized from normal on NaI to moderately abnormal on CZT, but this was due to an obvious truncation artifact on the latter. When scanning with CZT devices, it is imperative to place the patient's heart in the center of the quality field of view.[24,26] Although this can be difficult to achieve with large patients,[27] it can be accomplished with careful modified repositioning.[28] In the second case, a female patient scored as moderately abnormal on NaI was defined as normal on the CZT study. Review of the raw data and reconstructed results for the NaI study indicated the presence of a breast attenuation artifact.[29]

It has been suggested that the geometry of CZT cameras provides ray projections that pass through subdiaphragmatic soft tissue to the inferior row of pinhole collimators causing count loss in the inferior and inferolateral walls,[25] consistent with the diaphragmatic artifact often associated with male studies. Conversely, phantom studies indicate that the effects of breast attenuation in the anterior wall are somewhat ameliorated in CZT as compared to NaI.[25] This may be the basis for the gender-specific effects found in this study in which CTAC provided for a significant difference in MPI scoring for males but not females.

In present study, quantitation of diagnostic results of MPI-SPECT studies performed with a solid-state dedicated cardiac SPECT/CT camera, measured by SSS and SRS, resulted in significant changes with the application of CTAC when referenced to the appropriate database. Overall, the diagnostic category ''improved'' with CTAC, with the most common re-classification being from mildly abnormal to normal, further proof to the fact that when the appropriate custom database was used CT-based AC resulted in less attenuation artifacts and thus allowed for a more accurate assessment of the myocardial perfusion. The clinical consequences of a

Table 6. NAC and AC scoring averages for CZT grouped by BMI and type of stress

	BMI		Type of stress	
	<30 kg/m^2 (n = 93)	≥30 kg/m^2* (n = 59)	Pharmacological (n = 97)	Exercise[a] (n = 55)
SSS NAC	4.15 ± 6.33	4.10 ± 5.82	4.10 ± 5.74	4.18 ± 6.79
SSS AC	3.33 ± 5.33	3.71 ± 5.25	3.52 ± 5.34	3.42 ± 5.58
SRS NAC	2.25 ± 5.12	1.92 ± 4.35	2.01 ± 4.36	2.31 ± 5.60
SRS AC	1.61 ± 3.93	1.59 ± 3.84	1.55 ± 3.69	1.71 ± 4.24

SSS and SRS are expressed as mean ± SD
* No significant differences compared to < 30 kg/m^2
[a] No significant differences compared to Pharmacological

misclassification related to the use of an inappropriate database include potentially harmful use of unnecessary invasive procedures or applying an inadequate therapeutic strategy associated with inherent risks and costs.

The present study was limited to the comparison of automatically derived scores from MPI-SPECT and did not include angiographic or outcome data for the patient population. The generalizability of these findings to other solid-state detector cameras needs to be investigated. For example, a recent study demonstrated that a different, parallel-hole collimated CZT cardiac camera provided stress-only upright and supine NAC results that were non-inferior statistically to AC stress-only standard SPECT MPI, with possible reduced sensitivity for some readers, but AC CZT results were absent.[30] Also, further studies should be carried out in order to evaluate and monitor how a shift in the diagnostic category based on an AC-based change in SSS and SRS alters patient outcomes. Although predominately low risk scores may represent a typical clinical population, further analysis including more high risk scores might strengthen the findings in this study. In addition, this is a retrospective analysis of the effects of CTAC on MPI with relatively small cohorts at a single center. However, the present results underscore the need for custom-built databases to be used for CZT-MPI studies and warrant consideration toward continuing with a second phase to provide the level of confidence associated with large multi-center trials.

NEW KNOWLEDGE GAINED

A database comprising normal MPI results from standard SPECT MPI is insufficient for accurate SSS and SRS measurements with an ultrafast cardiac CZT SPECT/CT camera. A normal database referenced to the CZT camera should be used.

CONCLUSION

Using a specifically designed database for multi-pinhole solid-state CZT cardiac SPECT provides accurate quantitative diagnostic perfusion scores concordant with those previously validated for conventional SPECT. The need for a custom database was demonstrated by the fact that the same concordance was not achieved using solely the normal default database available for the conventional system. AC and NAC CZT scores differed significantly, especially in men.

Disclosures

Ora Israel is a consultant to GE Healthcare. No other author has any financial disclosures in relationship to this study.

References

1. Hendel RC, Berman DS, Di Carli MF, Heidenreich PA, Henkin RE, Pellikka PA, et al. ACCF/ASNC/ACR/AHA/ASE/SCCT/SCMR/SNM 2009 appropriate use criteria for cardiac radionuclide imaging. J Am Coll Cardiol. 2009;53:2201-29.
2. Hendel RC, Abbott BG, Bateman TM, Blankstein R, Calnon DA, Leppo JA, et al. ASNC information statement: The role of radionuclide myocardial perfusion imaging for asymptomatic individuals. J Nucl Cardiol. 2011;18:3-15.
3. Herzog BA, Buechel RR, Katz R, Brueckner M, Husmann L, Burger IA, et al. Nuclear myocardial perfusion imaging with a cadmium-zinc-telluride detector technique: Optimized protocol for scan time reduction. J Nucl Med. 2010;51:46-51.
4. Iskandrian AE. Stress-only myocardial perfusion imaging: A new paradigm. J Am Coll Cardiol. 2010;55:231-3.

5. Dorbala S, Di Carli MF, Delbeke D, Abbara S, DePuey EG, Dilsizian V, et al. SNMMI/ASNC/SCCT guideline for cardiac SPECT/CT and PET/CT 1.0*. J Nucl Med. 2013;54:1485-507.
6. Organisation for Economic Co-Operation and Development, Nuclear Energy Agency. The supply of medical radioisotopes implementation of the HLG-MR policy approach: Results from a self-assessment by the global $^{99}Mo/^{99m}Tc$ supply chain. The Supply of medical radioisotopes series 2013. http://www.oecdnea.org/med-radio/med-radio-series.html.
7. Bocher M, Blevis IM, Tsukerman L, Shrem Y, Kovalski G, Volokh L. A fast cardiac gamma camera with dynamic SPECT capabilities: Design, system validation and future potential. Eur J Nucl Med Mol Imaging. 2010;37:1887-902.
8. Ather S, Iqbal F, Gulotta J, Aljaroudi W, Heo J, Iskandrian AE, Hage FG. Comparison of three commercially available softwares for measuring left ventricular perfusion and function by gated SPECT myocardial perfusion imaging. J Nucl Cardiol. 2014;21:673-81.
9. Germano G, Kavanagh PB, Waechter P, Areeda J, Van Kriekinge S, Sharir T, et al. A new algorithm for the quantitation of myocardial perfusion SPECT. I: Technical principles and reproducibility. J Nucl Med. 2000;41:712-9.
10. Berman DS, Kang X, Gransar H, Gerlach J, Friedman JD, Hayes SW, et al. Quantitative assessment of myocardial perfusion abnormality on SPECT myocardial perfusion imaging is more reproducible than expert visual analysis. J Nucl Cardiol. 2009;16:45-53.
11. Nakazato R, Tamarappoo BK, Kang X, Wolak A, Kite F, Hayes SW, et al. Quantitative upright–supine high-speed SPECT myocardial perfusion imaging for detection of coronary artery disease: Correlation with invasive coronary angiography. J Nucl Med. 2010;51:1724-31.
12. Garcia EV, Folks RD, Raggi P, Keidar Z, Askew JW, Rispler S, et al. Quantitation of gated rest/stress Tc-99m tetrofosmin ultrafast CZT myocardial perfusion imaging: Development of normal limits and multicenter validation. The 15th Annual Scientific Session of the American Society of Nuclear Cardiology September 23-26, 2010. ASNC Abstracts. 2010;17:721.
13. Duvall WL, Slomka PJ, Gerlach JR, Sweeny JM, Baber U, Croft LB, et al. High-efficiency SPECT MPI: Comparison of automated quantification, visual interpretation, and coronary angiography. J Nucl Cardiol. 2013;20:763-73.
14. Sharir T, Pinskiy M, Pardes A, Rochman A, Prokhorov V, Kovalski G, et al. Comparison of the diagnostic accuracies of very low stress-dose with standard-dose myocardial perfusion imaging: Automated quantification of one-day, stress-first SPECT using a CZT camera. J Nucl Cardiol. 2016;23:11-20.
15. Hachamovitch R, Berman DS, Shaw LJ, Kiat H, Cohen I, Cabico JA, et al. Incremental prognostic value of myocardial perfusion single photon emission computed tomography for the prediction of cardiac death: Differential stratification for risk of cardiac death and myocardial infarction. Circulation. 1998;97:535-43.
16. Genovesi D, Giorgetti A, Gimelli A, Kusch A, D'Aragona Tagliavia I, Casagranda M, et al. Impact of attenuation correction and gated acquisition in SPECT myocardial perfusion imaging: Results of the multicentre SPAG (SPECT attenuation correction vs gated) study. Eur J Nucl Med Mol Imaging. 2011;38:1890-8.
17. Pourmoghaddas A, Vanderwerf K, Ruddy TD, Wells RG. Scatter correction improves concordance in SPECT MPI with a dedicated cardiac SPECT solid-state camera. J Nucl Cardiol. 2014;22:334-43.
18. Hendel RC, Berman DS, Di Carli MF, Heidenreich PA, Henkin RE, Pellikka PA. Appropriate use criteria for cardiac radionuclide imaging: A report of the American College of Cardiology Foundation Appropriate Use Criteria Task Force, the American Society of Nuclear Cardiology, the American College of Radiology, the American Heart Association, the American Society of Echocardiography, the Society of Cardiovascular Computed Tomography, the Society for Cardiovascular Magnetic Resonance, and the Society of Nuclear Medicine. J Am Coll Cardiol. 2009;53:2201-9.
19. Diamond GA, Forrester JS. Analysis of probability as an aid in the clinical diagnosis of coronary-artery disease. N Engl J Med. 1979;300:1350-8.
20. Hebert T, Leahy R. A generalized EM algorithm for 3D Bayesian reconstruction from Poisson data using Gibbs priors. IEEE Trans Med Imaging. 1989;8:194-202.
21. Green PJ. Bayesian reconstructions from emission tomography data using a modified EM algorithm. IEEE Trans Med Imaging. 1990;9:84-93.
22. Hudson HM, Larkin RS. Accelerated image reconstruction using ordered subsets of projection data. IEEE Trans Med Imaging. 1994;13:601-9.
23. Kennedy JA, Israel O, Frenkel A. Directions and magnitudes of misregistration of CT attenuation-corrected myocardial perfusion studies: Incidence, impact on image quality, and guidance for reregistration. J Nucl Med. 2009;50:1471-8.
24. Hindorf C, Oddstig J, Hedeer F, Hansson MJ, Jögi J, Engblom H. Importance of correct patient positioning in myocardial perfusion SPECT when using a CZT camera. J Nucl Cardiol. 2014;21:695-702.
25. Liu CJ, Cheng JS, Chen YC, Huang YH, Yen RF. A performance comparison of novel cadmium–zinc–telluride camera and conventional SPECT/CT using anthropomorphic torso phantom and water bags to simulate soft tissue and breast attenuation. Ann Nucl Med. 2015;29:342-50.
26. Kennedy JA, Israel O, Frenkel A. 3D iteratively reconstructed spatial resolution map and sensitivity characterization of a dedicated cardiac SPECT camera. J Nucl Cardiol. 2014;21:443-52.
27. Fiechter M, Gebhard C, Fuchs TA, Ghadri JR, Stehli J, Kazakauskaite E, et al. Cadmium-zinc-telluride myocardial perfusion imaging in obese patients. J Nucl Med. 2012;53:1401-6.
28. Gimelli A, Bottai M, Genovesi D, Giorgetti A, Di Martino F, Marzullo P. High diagnostic accuracy of low-dose gated-SPECT with solid-state ultrafast detectors: Preliminary clinical results. Eur J Nucl Med Mol Imaging. 2012;39:83-90.
29. DePuey EG. How to detect and avoid myocardial perfusion SPECT artifacts. J Nucl Med. 1994;35:699-702.
30. Jameria ZA, Abdallah M, Fernandez-Ulloa M, O'Donnell R, Dwivedi AK, Washburn E, et al. Analysis of stress-only imaging, comparing upright and supine CZT camera acquisition to conventional gamma camera images with and without attenuation correction, with coronary angiography as a reference. J Nucl Cardiol. 2017. doi:10.1007/s12350-017-0781-7.